Voprosy Onkologii = Problems in Oncology. 2026. Vol. 72, № 1
UDC 616-006.34
DOI 10.37469/0507-3758-2026-72-6-OF-2273

© *Sindudevi Jeevanandam, Muthaiya Govindarajan Kavitha*

Enhanced Residual Osteosarcoma Detection Using Deep Learning And Formularization Techniques On Histopathological Images

Department of Computer Science and Engineering, University College of Engineering Pattukkottai, Rajamadam, India

© *Дж. Синдудеви, Г.М. Кавита*

Усовершенствованное выявление резидуальной остеосаркомы с помощью методов глубокого обучения и формализации на гистопатологических изображениях

Кафедра компьютерных наук и инженерии, Инженерный колледж Университета Паттукоттаи, Раджамадам, Индия

Osteosarcoma has become increasingly prevalent globally in recent years, significantly impacting the mortality rates of those affected. Histopathological imaging plays a crucial role in the diagnostic process. The proposed research evaluates the effectiveness of these techniques in accurately detecting necrotic, non-viable, and viable tumors within histopathological tissue. The dataset underwent pretreatment using Gaussian filtering to enhance image quality, followed by formularization techniques to improve model generalization and reduce overfitting. Transfer learning models such as EfficientNetB6, DenseNet201, and MobileNetV2 were employed and trained on histopathological images to improve diagnostic accuracy. Pre-trained models derived from the ImageNet architecture were specifically applied for cancer detection. Additionally, a formularization technique was incorporated into the IGDOOD (Iterative gradient descent Of Osteosarcoma Detection) framework to mitigate overfitting and enhance model performance. Iterative gradient descent was the main optimization algorithm used for training the deep learning model, with the formularization techniques implemented to fine-tune the learning rate improve accuracy, and automatically capture tumor regions to extract the nuclear characteristics of tumor cells. These features to develop a histological image classifier for osteosarcoma, using IGDOOD to predict recurrence and survival rates post-treatment. Performance metrics be approximated to assess the efficiency of osteosarcoma detection with reported accuracy on test data being 95.02 % for EfficientNetB6, 99.10 % for DenseNet201, and 99.40 % for MobileNetV2.

Keywords: osteosarcoma; convolutional neural network; gaussian filtering; histopathological images; IGDOOD; MobileNetV2; EfficientNetB6; DenseNet201

For Citation: Jeevanandam Sindudevi, Govindarajan Muthaiya Kavitha. Enhanced residual osteosarcoma detection

В последние годы остеосаркома стала всё более распространённым заболеванием во всём мире, существенно влияя на показатели смертности среди пациентов. В процессе диагностики ключевую роль играет патогистологическая визуализация. В предлагаемом исследовании оценивается эффективность методов глубокого обучения в точном выявлении некротических, нежизнеспособных и жизнеспособных опухолей в патогистологических тканях. Набор данных был предварительно обработан с использованием метода фильтра Гаусса для улучшения качества изображений, после чего для повышения обобщающей способности модели и минимизации необходимости в переобучении были применены методы формализации. Для повышения диагностической точности использовались модели трансферного обучения, такие как EfficientNetB6, DenseNet201 и MobileNetV2, обученные на патогистологических изображениях. Для выявления рака применялись предварительно обученные модели, полученные на основе архитектуры ImageNet. Кроме того, метод формализации был интегрирован в структуру IGDOOD (метод итеративного градиентного спуска для обнаружения остеосаркомы) для снижения необходимости в переобучении и улучшения работы модели. Итеративный градиентный спуск — это основной алгоритм, который применялся для оптимизации, во время подготовки модели глубокого обучения; методы формализации использовались для тонкой настройки скорости обучения, повышения точности и автоматического определения областей опухоли для извлечения ядерных характеристик опухолевых клеток. На основе этих характеристик был создан классификатор гистологических изображений для остеосаркомы, использующий IGDOOD для прогнозирования показателей рецидива и выживаемости после лечения. Эффективность обнаружения остеосаркомы оценивалась с помощью метрик производительности, согласно которым точность на тестовых данных составила: для EfficientNetB6 — 95,02 %, для DenseNet201 — 99,10 % и для MobileNetV2 — 99,40 %.

Ключевые слова: остеосаркома; сверточная нейронная сеть; фильтр Гаусса; патогистологическая визуализация; IGDOOD; MobileNetV2; EfficientNetB6; DenseNet201

Для цитирования*:* Дж. Синдудеви, Г.М. Кавита. Усовершенствованное выявление резидуальной остеосаркомы

using deep learning and formularization techniques on histopathological images. *Voprosy Onkologii = Problems in Oncology*. 2026; 72(1): 00-00.-DOI: 10.37469/0507-3758-2026-72-1-OF-2273

с помощью методов глубокого обучения и формализации на гистопатологических изображениях. *Вопросы онкологии*. 2026; 72(1): 00-00.-DOI: 10.37469/0507-3758-2026-72-1-OF-2273

✉ Contact: Sindudevi Jeevanandam, jsindudevi87@gmail.com

Introduction

The American Cancer Society projects that in 2024, it is projected that there will be approximately 2,001,140 new cancer cases and 611,720 deaths referable to cancer in the United States. Among these, osteosarcoma — a rare malignant bone tumor — poses significant challenges due to its impact on mortality rates [1]. Despite advancements in a from 2000 to 2022 indicate a persistent need to improve the five-year survival rate for osteosarcoma patients. These statistics underscore the critical need for advancements in diagnostic methodologies, particularly for rare cancers like osteosarcoma [2]. Osteosarcoma is classified as a rare cancer, with the International Agency for Research on Cancer (IARC) reporting around 430 global cases annually, and an incidence rate of 0.5 per million. The five-year survival rate remains between 50 and 60 %, with IARC projecting around 340 new cases and 220 deaths from osteosarcoma in 2024. Notably, 10 % of these cases occur in individuals aged 60 and above, and osteosarcoma accounts for approximately 2 % of cancer diagnoses in children. Early detection remains crucial, as the mortality rate is significantly elevated when the disease is not caught early [4]. A machine learning framework was developed, incorporating image processing and support vector machines (SVM) to detect infections and classify cancer types. The researchers determined that SVM performed optimally for bone prognosis. This paper conducted two experiments, one utilizing hog feature sets and the other without, applying an Unpredictable forest and Classification algorithm. The operation of these models was evaluated using 5-fold cross-validation [5], a machine learning methodology aimed at identifying tumor-influenced regions within histopathological images of bone. The authors utilized morphological classification alongside recurrent convoluted neural networks (RCNN) for image analysis. This investigation advances the creation of AI-driven diagnostic tools for bone tumors, which may enhance diagnostic precision and patient results [6]. To improve the precision of image classification through (CNNs), a class of algorithms. This study plays a significant role in advancing AI-supported diagnostic tools in medical imaging [7]. Osteosarcoma is a type of bone cancer that predominantly affects adolescents and young adults, accounting for approximately 60 % of all malignant bone tumors diagnosed in individuals before reaching young adulthood. This particular cancer exhibits a peak incidence during puberty, a critical period of growth and development, which may contribute to its prevalence in this age group [8]. Sarcoma becomes a type of tumour that develops in the bones. The ordinary location is in the arms and legs, particularly around the knee or hips., Osteosarcoma occurs most often in people around 30. Early detection and treatment are crucial to improve the five-year survival rate, around 70 %. Chemotherapy, surgical resection, and radiation therapy are the primary treatment options. [9]. Extracting quantitative features from tumor nuclei using histopathological images stained with hematoxylin and eosin (H&E)/Features are then used to train a classifier that can accurately predict outcomes, potentially aiding in personalized treatment planning and improving patient prognosis [11]. Integrating the remora optimization algorithm improves the model's performance by optimizing parameters and enhancing classification. The proposed model demonstrates high accuracy in detecting and classifying osteosarcoma, making it a promising tool for early diagnosis and treatment planning [12]. The prognosis of osteosarcoma is based on several factors most notably the stages of the cancer at diagnosisand the presence or absence of metastases. Relapses are likely to occur within a first few years after intial treatment. The importance of this research is highlighted by its capacity to provide an automated and accurate diagnostic solution a tool for osteosarcoma, which can significantly reduce the diagnostic burden on pathologists and improve patient outcomes. Despite the promising results, several challenges remain, including the variability in image quality, the computational resources required for model training, and the ethical and logistical considerations of integrating these advanced techniques into clinical practice.

This research developed a fully automated process for extracting quantitative features from histopathology images and evaluated their diagnostic significance in osteosarcoma. We created classifiers to predict outcomes and identified unique image features linked to recurrence, validating these in an independent cohort. The osteosarcoma histological image classifier(S) helps identify patients who may benefit from standard treatment, offering crucial prognostic information for those diagnosed with osteosarcoma.

The main objectives of this research are:

1. This study aims to demonstrate that deep learning-based tools can accurately identify osteosarcoma using a publicly available set of data. The aim towards effectively identify between the average characteristics of Nonviable tumor, necrosis, tumors, and viable cancer tissues.

2. Find the Osteosarcoma with a high level of accuracy detection using deep learning models such as MobileNetV2, DenseNet201, and EfficientNetB6. The dataset is collected from the open source of trained images, afterward, fine-tune the model along with its features and classify the necrosis, viable tumor, and non-viable tumor and attain high accuracy. Furthermore, the research intends to identify an appropriate predictive modeling algorithm that guarantees exact identification and explore potential characteristics to enhance performance.

To accomplish these main objectives, cytological medicinal picture analysis was performed using transfer learning techniques on a specified dataset. Three modified meta learning models — MobileNetV2, DenseNet201, and EfficientNetB6 — were utilized for data analysis. The innovative aspect of this approach is its application across various categories within the dataset while employing the entire tile image as input.

The subsequent sections of this paper are structured as follows: Section 2 provides a brief overview summary of research related to the classification of osteosarcoma images. Section 3 describes the methodologies used in this study. Section 4 elaborates on the implementation approach. Section 5 showcases the results achieved. Finally, Section 6 covers the paper with a conclusion and future work.

Literature Review

A Model utilizing a Siamese Network (DS-Net) has been developed. to address various challenges in medical image classification. This classification network utilizes features extracted by the Advanced Siamese Network (ASN), leading to more precise classification outcomes. Many existing deep learning methods focus on simpler models to mitigate the risk of overfitting, particularly when working with small datasets. Unfortunately, this approach often results in poor feature extraction and reduced accuracy [16]. In addition, Paper [17] discusses insights from a study conducted by Chen et al., highlighting the importance of utilizing models of femoral bone tumors. This aligns with the ongoing advancements in computational techniques in pathology, emphasizing how these tools can enhance diagnostic accuracy and improve patient outcomes. By integrating sophisticated models, healthcare professionals can better differentiate between tumor types, leading to more effective treatment plans tailored to individual patient needs. Paper [19] introduces a fully automated segmentation method for spinal MRI images utilizing a convolutional-deconvolutional neural network and a patch-based deep learning approach. This method aims to enhance segmentation efficiency and accuracy, fulfilling clinical requirements for precise diagnosis and treatment planning. The improved delineation of spinal structures is expected to assist healthcare professionals in making more informed clinical decisions.

Various researchers demonstrate the technology of expert system for identification of tumour, particularly focusing on osteosarcoma, a type of bone cancer. They use medical images from X-rays and CT scans to identify osteosarcoma. The traditional and time-consuming biopsy method is suggested to be automated. They apply several supervised learning methods such as VisualGeometryGroups16 (VGG16), VisualGeometryGroups19 (VGG19), Dense ConvolutionalNetwork201 (DenseNet201), and Residual Neural Network101 (ResNet101) augmented with ANN layers through transfer learning. The results are promising, with the ResNet101 algorithm achieving the highest accuracy at 90.36 and 89.51 % precision in prediction tasks [20]. Paper [22] described The identification of different types of brain tumors has been conducted. In the two experiments, the proposed network architecture yielded impressive outcomes, achieving an overall accuracy of 96.13 percent and 98.7 percent, respectively. The results demonstrated that the proposed methodology effectively detects various types of brain tumors. The transfer learning techniques, specifically VGG16, EfficientNetB5, ResNet50, and DenseNet169, to identify and classify osteosarcoma from histopathology images. The study utilizes pre-trained convolutional neural networks on a public dataset to categorize the appearance into viable, non-tumor, and tumor classes. Leveraging weights from the ImageNet model in the convolutional models, with transfer learning and a fully connected layer, the research successfully handles a three-class label system [23]. Presents a system that combines features extracted through traditional handcrafted methods and advanced deep learning architectures, particularly EfficientNet-B0 and Xception. Enhance performance, Two binary variants of the Arithmetic Optimization Algorithm (AOA), referred to as BAOA-S and BAOA-V, have been developed for the purpose of feature selection in tumor (NVT) and non-tumor (NT) categories. 24]. Remarkably, the implementation of BAOA-S for feature selection achieved an overall accuracy of 99.54 % while reducing the number of features from 2118 to 188.The paper [25] described that the model further incorporates Inception v3, a pre-trained deep learning architecture, for feature extraction. Increasing the Inception v3 model, the

Owl Search Algorithm is employed for adjustment parameter optimization. Additionally, Long Short-Term Memory (LSTM) networks are utilized to detect bone cancer. This multi-faceted approach aims to improve accuracy and effectiveness in cancer detection. The application of sophisticated computational methods in pathology has revolutionized how healthcare professionals examine and interpret intricate tissue specimens. Deep learning algorithms, especially convolutional neural networks (CNNs), have demonstrated significant potential in identifying osteosarcoma from histopathological images. This study illustrates that machine learning has the potential to enhance diagnostic accuracy and lower healthcare costs related to advanced imaging technologies. Paper [27] proposed this study introduces an osteosarcoma MRI image segmentation method known as OSTransnet, which is founded on Transformer and U-net architectures. The proposed technique specifically targets the challenges associated with unclear tumor edge segmentation and the overfitting caused by data noise. Initially, we enhance the dataset by modifying the spatial distribution of noise and implementing a data-increment image rotation process. Paper [15] proposes that the presence of osteosarcoma can be accomplished through transfer learning using pre-trained models. Additionally, Paper [13] underscores the genetic and biomolecular resemblances between canines and humans, particularly concerning changes in gene expression and specific microRNAs. This finding highlights the potential for cross-species insights to enhance the understanding of osteosarcoma, thereby contributing to more effective treatment and diagnostic strategies in veterinary and human medicine.

Suggested Technique

The suggested technique consists of many ways data pretreatment. Extract characteristics and Consignment. The concept involves utilizing the weights obtained from an earlier model to address new challenges, a process known as “transfer learning. To get a definite and enhance its efficiency by diminishing the aggregating capacity, using deep learning models, DenseNet201, Efficient NetB6, and MobileNetV2 have been used in this work to classify osteosarcoma with three grades (Non-viable tumor, viable tumor, and Necrosis). Osteosarcoma is a type of primary malignant bone tumor that comes in several histological variants. The conventional type is the most prevalent, making up about 75 % of all cases. It includes subtypes like osteoblastic, chondroblastic, and fibroblastic.

The database is pre-processed using Python tools, followed by feature extraction through convolutional neural network (CNN) methods. Various CNN approaches have been employed to compare and classify the images. Fine — tune the learning rate by employing the formularization strategies the model’s efficiency in detecting osteosarcoma. The improvement and judgement of the miniature are conducted after these steps. Fig. 1 illustrates the flow diagram of the proposed approach.

Dataset

A comprehensive overview of the image set and the methodology employed is provided in the subsequent subsections. The research utilized the publicly available Osteosarcoma dataset from UT Southwestern/UT Dallas, which focuses on evaluating viable and necrotic tumors. This dataset includes histological images of osteosarcoma samples with hematoxylin and eosin (H&E). The excised bone tissue was processed by cutting it into fragments, demineralizing, staining with H&E, and preparing it as slides. The image set is divided into three parts: 80 % for the training set, 20 % for the validation set, and 20 % for the testing set. The dataset comprises of 1100 histopathology images consisting of the following distributions (50 %non-tumor, 20 % necrotic tumor images, and 30 % viable tumor tiles). The dark red area stained with immature woven bone or

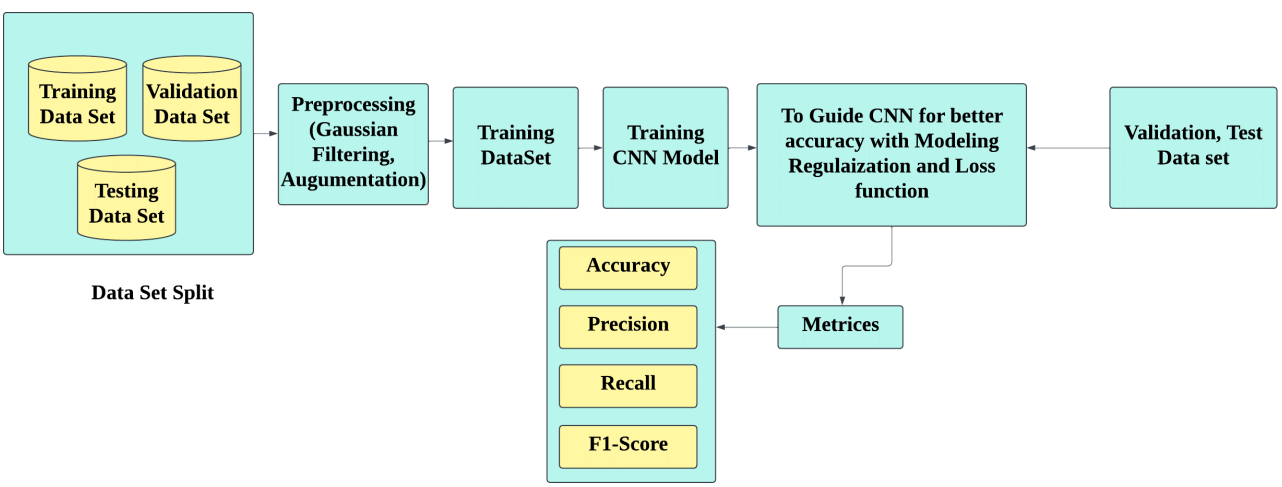

Fig 1. Proposed Methodology

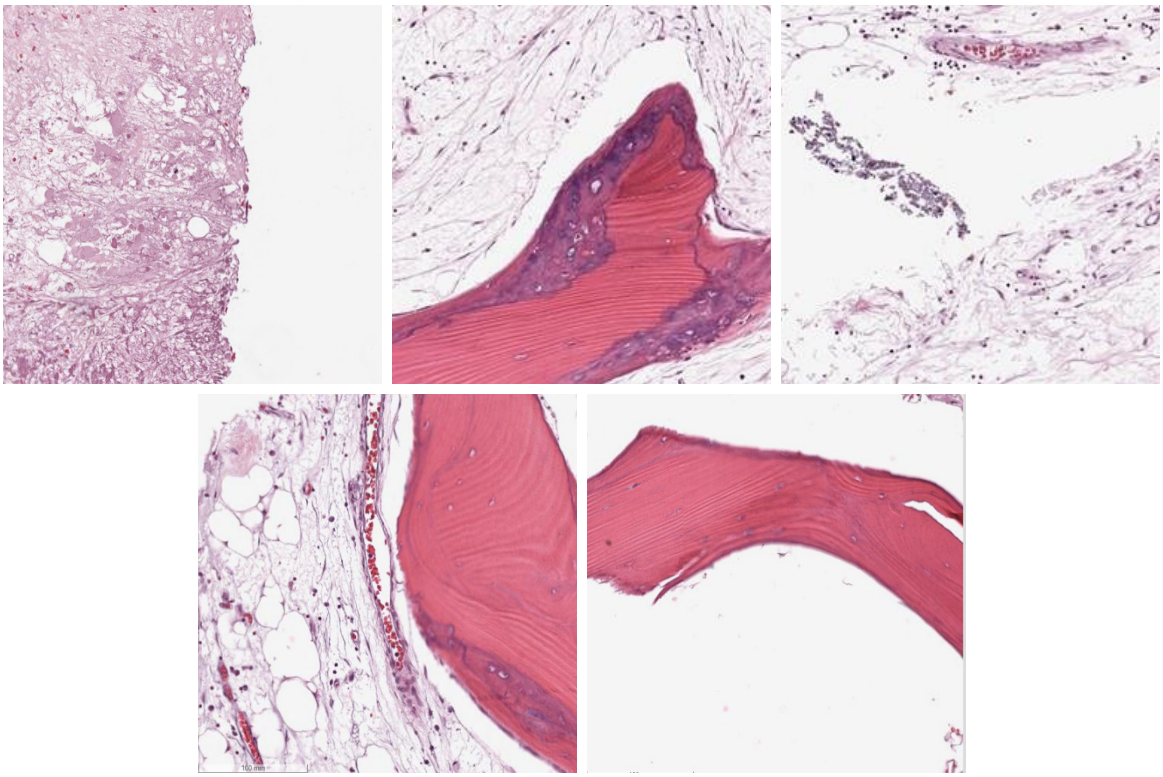

Fig 2. Histopathological images of viable, and non-viable tumor

osteoid, which is a characteristic feature of osteosarcoma. The adjacent cellular area is populated with spindle-shaped cells and nuclei that appear active. There is no discernible cartilaginous matrix present (which would suggest chondroblastic osteosarcoma). No significant large hemorrhagic or cystic spaces are evident (which are typically observed in the telangiectatic type). There is an absence of a dense fibrous matrix that would dominate the field (as seen in the fibroblastic type). Osteoblastic Osteosarcoma: This subtype is the most prevalent, and based on the observation of Prominent osteoid (immature bone matrix) and Active bone-producing tumor cells, it aligns visually with osteoblastic osteosarcoma.

Based on the visual characteristics of the histopathological images — particularly the presence of dense eosinophilic osteoid regions and osteoblast-like cells — the samples are consistent with features of the osteoblastic subtype of osteosarcoma. However, as the dataset does not provide subtype-level labels, this categorization is used only for observational reference and not as a confirmed histopathological diagnosis.

Pretreatment

The pre-treated images are applied to the proposed methodology to achieve effectiveness. The proposition composed definite and adequate impact correlated to the barrier methods. Image processing methods including color, texture, and structure are selected aspects. The image size is 1024 ×1024 pixels. An illustraton of the assize to 128 × 128 pixels.

Aspects including color, texture, and structure by pretreatment. The illustration of the extent within the dataset are 1024 × 1024 pixels. Each image is subsequently resized to 128 × 128 pixels. The pretreatment includes the image enhancement steps, e.g. data augmentation and normalization. The procedure applicable to the data augmentation method previously discussed concerning the data set is elaborate. Histopathology images are rotated, such a transformation was used of the two in the training and testing phases.

Gaussian Filtering

A Gaussian filter is linear commonly employed in computer vision to enhance image smoothness. Reduce the noise level from the image dataset It's called a Gaussian filter because it uses a Gaussian function (bell- shaped curve) to weigh the pixels, getting more significant to the central pixels and less to those further away. The Gaussian Filter (GF) method is a critical step in image pretreatment, specifically designed to eliminate unwanted noise from images. The Gaussian Filter is a well-established and widely utilized technique in image processing, recognized

for its effectiveness in enhancing image quality. GF involves convolving an image with a Gaussian function. This convolution enables some degree of noise to be deleted, while still showing the characteristics of the region that has been selected regarding the image. It is commonly employed for noise reduction, it helps to create clear pictures by smoothing out fluctuations.

Formularization

Formularization is crucial in machine learning to prevent overfitting by penalizing model coefficients in deep learning,

The focus is on weight matrices, with L1 (Lasso) and L2 (Ridge) formularization techniques being commonly used.

The cost function is adjusted by adding a formularization term to mitigate overfitting, and techniques such as L2 formularization (weight decay) and dropout are utilized. The initial weights are represented as follows:

$$I = i1,\ i2,\ i3,\ \ldots\ldots\ldots \text{ in (I- Weight)} \quad (1)$$

And,

$$g = g1,\ g2,\ g3,\ \ldots\ldots\ldots\ gn \quad (g \text{ — given Bias}) \quad (2)$$

The output is represented in approximate manner is A

$$A = i1\ x1\ +i2\ x2\ +\ldots\ldots+in\ xn,\ +\ g \quad (3)$$

L1 formularization (Lasso)

$$L1\ \text{loss} = \text{Loss} + \text{factor} * \sum \quad (4)$$

L2 formularization (Ridge):

$$L2\ \text{Loss} = (1/n) * \Sigma\ (y\_true - y\_pred)\ \hat{}\ 2$$

In these formulas, λ is the formularization parameter, and i indicates the weights formularization improves a model's generalization to unseen data by applying uniform penalties, resulting in smaller coefficient values. Tuning λ balances the original loss and formularization, optimizing performance. It enhances the cost function by combining Categorical Cross-Entropy with a formularization term.

A defining characteristic of L1 formularization is its imposition of penalties based on the absolute values of the weights, which allows for the possibility of some weights being exactly zero. This feature makes L1 formularization particularly advantageous by reducing their associated weights to zero.

When applying this formularization technique in deep learning models, one must choose between L1 (Lasso) and L2 (Ridge) formularization. L1 is Valuable for feature selection due to its ability to potentially set some coefficients to zero, whereas L2 tends to retain all features while shrinking their values. To incorporate the formularization term into the model's cost function, for L1 formularization, include the total of the complete values augmented through a formularization values.

For L2 formularization, include the total quared values augumented through lambda. Techniques such as cross-validation can be employed to determine the optimal lambda. Utilize your training data to fit the model with the adjusted cost function, ensuring that formularization is applied to mitigate overfitting by penalizing complex models.

After training, evaluate the model using validation data to determine if formularization has enhanced its generalization capabilities to new or unseen data. Adjusting lambda or modifying the model architecture may further improve performance. Incorporating formularization techniques into your research on osteosarcoma detection is crucial for developing model robustness. After implementing these modifications, compile your models and start the training process. Monitor your validation metrics to ensure that formularization is effectively reducing overfitting. Adjust the lambda value for L2 formularization and the dropout rate is based on your specific dataset and task performance. Experiment with various dropout rates and L2 penalties to identify the optimal configuration.

A hyperparameter governs the equilibrium between the original loss and the formularization term, commonly represented as lambda (λ), which dictates the intensity of the formularization effect. By fine-tuning these values, practitioners can identify the optimal degree of formularization that improves the model's performance on unseen data.

Finally, formularization is a basic approach in machine learning and deep learning that enhances the cost function by incorporating both the loss from Categorical Cross-Entropy and a formularization term, for a detailed analysis of the components involved in the formulation. This one yields a penalty with the smallest cost function. By L2 formularization it shrinks when it does not reduce the weights to zero while diminishing. On the other hand, L1 formularization functions in different ways. A defining feature of L1 formularization is that it imposes penalties based on the absolute values of the weights, allowing for the possibility that some weights may be exactly zero. This characteristic makes L1 formularization particularly effective for feature selection, as it can successfully eliminate less significant features by reducing their corresponding weights to zero.

Aggregation

After the formularization process optimizing the given procedure is an important element in the machine learning model, as it significantly affects the model's capacity to learn from data and enhance its performance. There are many Notable optimization algorithms including Iterative Gradient Descent, Iterative Gradient Descent (IGD) is frequently utilized in the training of Convolutional Neural Network (CNN) models.

One of the advantages of IGD is its capacity for more frequent updates to the model parameters. This feature is particularly advantageous when dealing with large datasets, to get faster convergence while using large datasets toward an optimal solution. To increase the model's exploration and degree of randomness and speed up the training process.

Frequent steps are taken to minimize the loss function. IGD increases the chances of identifying a more optimal global minimum, ultimately leading to enhanced model performance.

Loss function

The loss function is essential for training deep learning models, particularly convolutional neural networks (CNNs). The measure assesses the disparity between the model's predictions and the actual target labels, providing a systematic way to evaluate model performance. During training, the model's predictions are compared to true labels, and the loss function calculates a numerical error value. This error is crucial for the backpropagation algorithm, which adjusts the model's parameters.

Backpropagation uses the gradient of the loss function to the model's weights to guide weight updates aimed at reducing loss. Higher loss values indicate greater discrepancies, offering feedback for optimizing future training iterations. A well-defined loss function is vital for optimal model performance; without it, the model lacks a clear optimization goal, hindering learning. The loss function balances the data during backpropagation. It is essential for improving model performance, which is critical for achieving accurate predictions. The choice of loss function significantly impacts training, including convergence speed and overall performance, with different functions suited for tasks selecting an appropriate loss function is to align the fitting model.

Implementation Details

Architecture

The Convolutional Neural Network (CNN) is a specialized type of deep learning architecture (DenseNet201, EfficientNetB6, MobileNetv2) that is particularly effective for tasks involving image classification and prediction.

A 128 x 128 image size with 3 channels is pretty standard and your choice of layers and activations seems solid. The design of a CNN is characterized by a series of layered components, each serving a distinct purpose in the processing of visual data. This layered approach allows the network to automatically learn and extract hierarchical features from images, for achieving high accuracy in classification tasks. Before the images are fed into the fully connected layers of the network, both the training and testing datasets undergo a series of pretreatment steps. These steps include the application of kernel filters, which are small matrices that slide to find various features such as edges, structure, textures, and patterns. This process is known as convolution, and it helps the network to learn and identify the features. Additionally, max-pooling layers are employed to down-sample the feature maps generated by the convolutional layers. Max-pooling reduces the dimensionality of the data while retaining the most important information, which helps to minimize computational load and reduce the risk of overfitting.

In the hidden layers of the CNN, the Rectified Linear Unit (ReLU) activation function is used ReLU introduces non- linearity into the model, allowing it to learn complex patterns in the data. This is done by outputting the input directly if it is positive; otherwise, it outputs zero helps to accelerate the training process, and improves the overall performance of the network.

The use of ReLU across all three hidden layers ensures that the model can effectively capture and represent intricate relationships within the data. For the final output layer, the SoftMax activation function is applied. SoftMax transforms the raw output scores of the network into probabilities that sum to one, making it particularly suitable for multi-class classification problems. This function allows the model to predict the values and facilitate the identification of the most probable class. Fig 3 shows the validation and training loss and accuracy of the deep learning models with epoch values.

Performance Metrics

To evaluate the CNN models, a range of measures are employed, containing Recall, Precision, F1-score, and accuracy. For its evaluation, deep learning models apply these metrics. After applying these to detect the accuracy, whether it's correct or not. Recall assessment evaluates the model's capacity to recognize all pertinent instances., while Precision assesses the precision of the model's positive predictions through the F1 score, which serves to balance Precision and Recall, thereby providing a unified metric. the model's overall performance. Accuracy, on the other hand, indicates The ratio of accurate predictions generated by the model relative to the overall total. predictions. By analyzing these metrics, practitioners can gain insights into the strengths and weaknesses of different models. Calculate the metrics values

$$\text{Accur} = \frac{\text{TruePos} + \text{TrueNeg}}{\text{Truepos} + \text{TrueNeg} + \text{FalsePos} + \text{FalseNeg}} \quad (6)$$

$$\text{Precis} = \text{TruePos} \qquad \text{Truepos} + \text{FalseNeg} \quad (7)$$

$$\text{Recal} = \frac{\text{TruePos}}{\text{Truepos} + \text{FalseNeg}} \quad (8)$$

$$\text{F1} = \frac{2*\text{preci} *\text{recall}}{\text{Preci}* + \text{recall}}$$

True Positives (Tp): This metric represents the count of the cases in which the model finds out in positive class

Table1. Trainable and Nontrainable parameters of the CNN model

	Total Parameters	Trainable Parameters	Non-Trainable Parameters
DenseNet201	41,552,793	41,328,354	224,439
EfficientNetB6	40,960,140	40.730,700	2,29,400
MobileNetV2	2,588,490	2,554,378	34,112

Table 2. Pre-trained CNN models accuracy Model

	Training set	Validation set	Testing set
DenseNet201	98.90	99.50	99.10
EfficientNetB6	94.50	96.00	95.02
MobileNetV2	98.60	99.65	99.40

DenseNet201

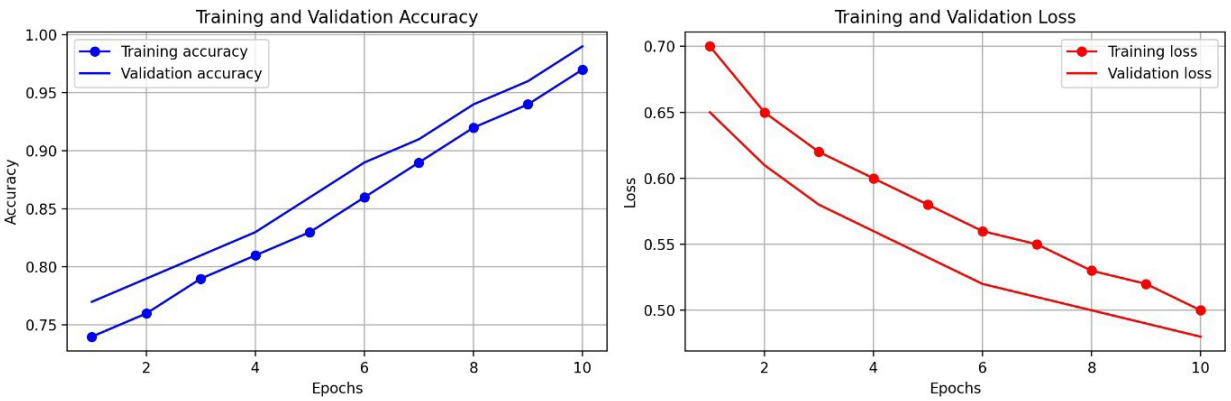

EfficientNetB6

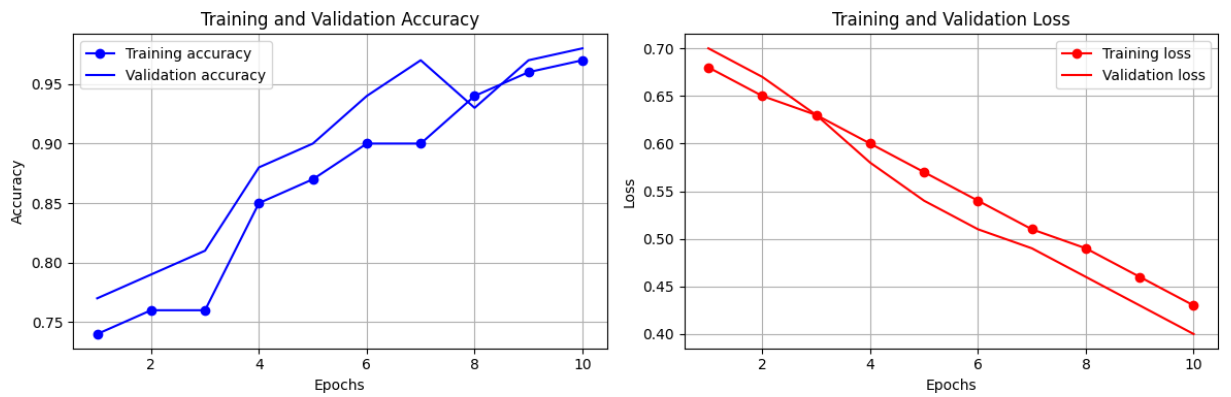

MobileNetV2

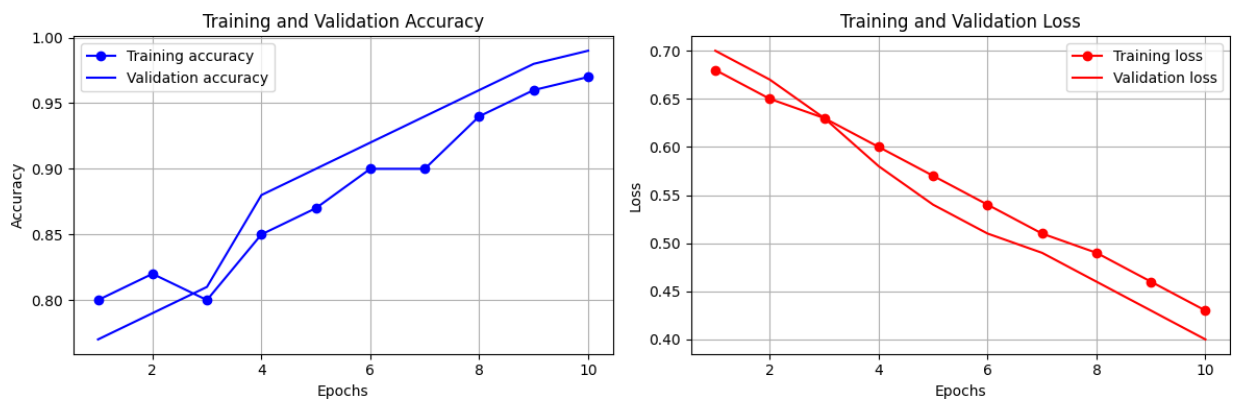

Fig 3. Validation and training loss and accuracy

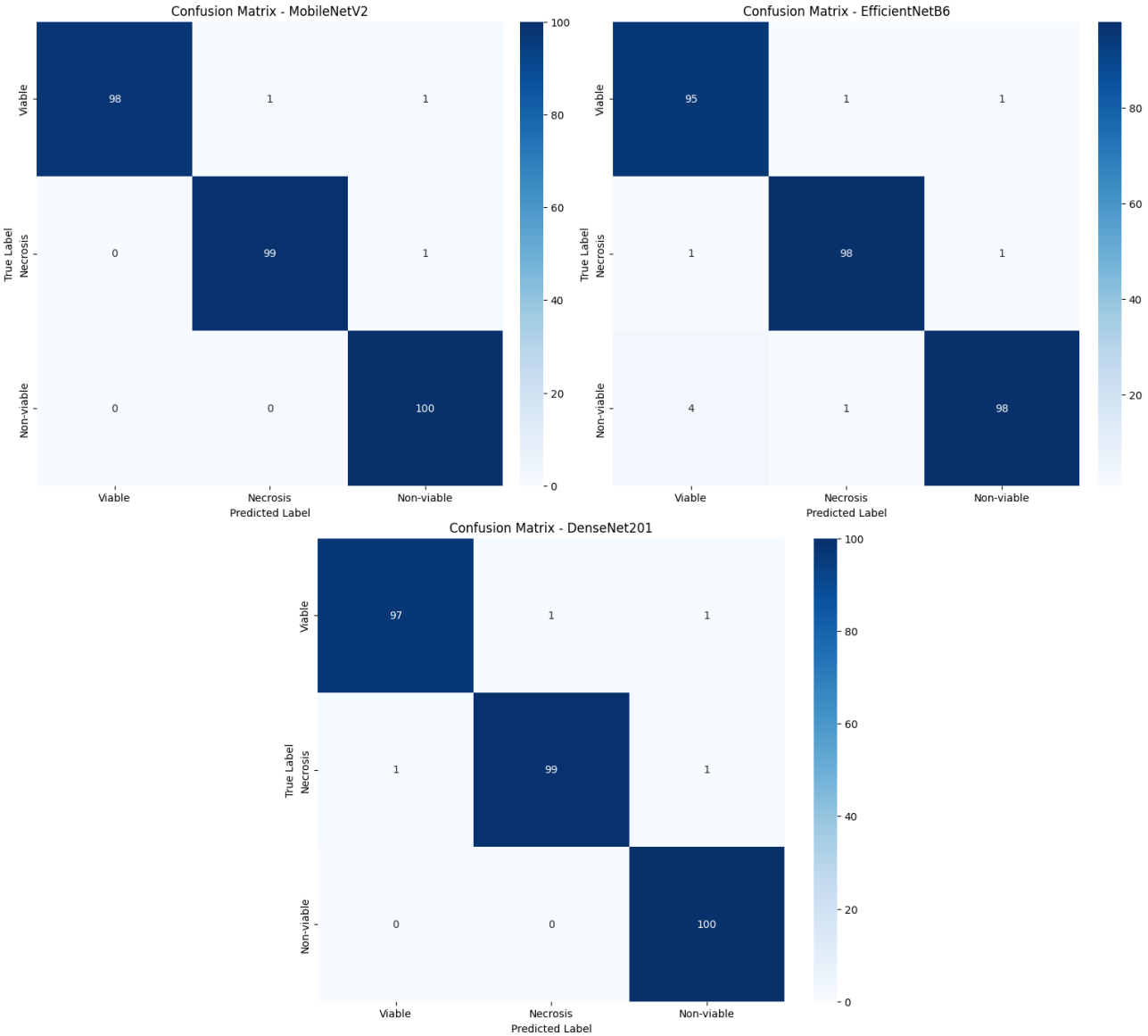

Fig 4. Confusion matrix

True Negatives (Tn): This metric reflects the count of the cases that accurately predict the negative class False Positives (Fp): This metric indicates count of the cases in which the method inaccurately find out the positive class False Negatives (FN): Indicate the count of the cases incorrectly predicts the gloomy class these four metrics—true positives, true negatives, false positives, and false negatives—are essential for assessing the performance of a classification model.

Result and Discussion

The estimation measure in favour of all orders using the three models are the subsequent sections provide a summary of the findings. Figure 3 illustrates the confusion matrix for all classifications conducted using the networks. Table 1 Trainable and Non- trainable parameters of CNN model Table 2 displays the pre-trained CNN accuracy models of training, validation, and testing sets of deep learning models.

The learning of pre-trained models in this study to analyze and plot the confusion matrix. The accuracy and loss metrics for each epoch during both training and validation phases, utilizing a balanced dataset, are illustrated in Figure 3. Models are trained using a given dataset set of training images, and the models are then validated with fine-tuning of parameters by applying the formularization technique. Every layer's weight in the models is maintained at the same level as the base model by following the idea of transfer learning. The performance outcomes of all models trained utilizing this technique.

Table 1 shows the parameters listed in the three deep-learning models. With the outcome of obtained tailores pre-trained models, evaluate the accuracy of each model. MobileNetV2 demonstrates the best performance, in terms of accuracy (99.40 %).

Secondly represents DenseNet201 (99.10 %). The least one gets (95.02 %) is EfficientNetB6. A model gets great performance under the comparative analysis. The comparisons and analysis have been undertaken to choose the model with the greatest performance. The following illustrates the confusion matrix of the deep learning model.

Fig. 4 shows the confusion matrix for necrosis, Viable tumor, and Non-Viable Tumor employing Pre-trained models are evaluated based on the metrics of precision, recall, and F1 Score for the proposed model. Each of the models generates a considerable volume of output. DenseNet201 acquired accuracy results reached as high as 99 %. EfficientNetB6 achieves an average accuracy of 95.02 %, the lowest mid of all pre-trained models. In contrast, MobileNetV2 demonstrates an average accuracy of 99.40 % while maintaining the shortest execution time. Additionally, average precision and recall metrics were calculated. F1_score achieved for the categorization of cancer subtypes.

Conclusion And Future Work

Osteosarcoma outcomes in unusual augmentation occur in bones increase, in this case, influences the other components. An approach employs a feature fusion technique with deep learning models, specifically EfficientNetB6, MobileNetV2, and DenseNet201, and predicts osteosarcoma by employing training and testing images. Results show MobileNetV2 attained an impressive test accuracy of 99.40 %, with EfficientNetB6 and DenseNet201 achieving accuracies of 95.02 and 99.10 %,

respectively. It indicates that the accuracy of convolutional neural network (CNN) models can be significantly improved through careful hyperparameter optimization. Notably, the application of formularization techniques has enhanced the models' effectiveness. While pre-trained models exist, they require fine-tuning to achieve specific performance goals. MobileNetV2 exhibited a shorter execution time and demonstrated rapid convergence. In the future, we plan to explore other deep-learning models that can deliver similar performance while being more computationally efficient. This investigation aims to reduce computational requirements improve system processing speed, and be effective.

Conflicts of interest
The authors declare no conflict of interest.

Funding
Self-funded. No external funding.

REFERENCES

1. Siegel R.L., Giaquinto A.N., Jemal A. Cancer statistics, 2024. CA Cancer J Clin. 2024; 74(1): 12-49.-DOI: https://doi.org/10.3322/caac.21820. Erratum in: CA Cancer J Clin. 2024; 74(2): 203.-DOI: https://doi.org/10.3322/caac.21830.
2. Yin C., Chokkakula S., Li J., et al. Unveiling research trends in the prognosis of osteosarcoma: A bibliometric analysis from 2000 to 2022. Heliyon. 2024; 10(6): e27566.-DOI: https://doi.org/10.1016/j.heliyon.2024.e27566.
3. Global Cancer Observatory — World Health Organization. International Agency for Research on Cancer (IARC). 2025.-URL: https://gco.iarc.fr/en.
4. Sharma A., Yadav D.P., Garg H., et al. Bone cancer detection using feature extraction machine learning model. *Comput Math Methods Med*. 2021; 2021: 7433186.-DOI: https://doi.org/10.1155/2021/7433186.
5. Anand D., Arulselvi G., Balaji G.N. Detection of tumor affected part from histopathological bone images using morphological classification and recurrent convoluted neural networks. *Journal of Pharmaceutical Negative Results*. 2022; 4992–5008.-DOI: https://doi.org/10.47750/pnr.2022.13.s09.617.
6. Ahmed I., Sardar H., Aljuaid H., et al. Convolutional neural network for histopathological osteosarcoma image classification. *Computers, Materials & Continua*. 2021; 69(3): 3365–81.-DOI: https://doi.org/10.32604/cmc.2021.018486.
7. Belayneh R., Fourman M.S., Bhogal S., et al. Update on osteosarcoma. *Curr Oncol Rep.* 2021; 23(6).-DOI: https://doi.org/10.1007/s11912-021-01053-7.
8. 8. Wang Z., Lu H., Wu Y., et al. Predicting recurrence in osteosarcoma via a quantitative histological image classifier derived from tumour nuclear morphological features. *CAAI Transactions on Intelligence Technology*. 2023; 8(3): 836–48.-DOI: https://doi.org/10.1049/cit2.12175.
9. 9. LeCun Y., Bengio Y., Hinton G. Deep learning. *Nature.* 2015; 521: 436–444.-DOI: https://doi.org/10.1038/nature14539.
10. Chen X., Chen H., Wan J., et al. An enhanced AlexNet-Based model for femoral bone tumor classification and diagnosis using magnetic resonance imaging. *J Bone Oncol*. 2024; 48: 100626.-DOI: https://doi.org/10.1016/j.jbo.2024.100626.
11. Chhabra P., Kumar R., Prasad R., et al. Osteosarcoma cancer detection using machine learning techniques. *Innovations in Data Analytics*. 2024; 13–28.-DOI: https://doi.org/10.1007/978-981-97-4928-7_2.
12. Chen W., Han Y., Awais Ashraf M., et al. A patch-based deep learning MRI segmentation model for improving efficiency and clinical examination of the spinal tumor. *J Bone Oncol*. 2024; 49: 100649.-DOI: https://doi.org/10.1016/j.jbo.2024.100649.
13. Gawade S., Bhansali A., Patil K., Shaikh D. Application of the convolutional neural networks and supervised deep-learning methods for osteosarcoma bone cancer detection. *Healthcare Analytics*. 2023; 3: 100153.-DOI: https://doi.org/10.1016/j.health.2023.100153.
14. Talukder Md.A., Islam Md.M., Uddin Md.A., et al. An efficient deep learning model to categorize brain tumor using reconstruction and fine-tuning. *Expert Systems with Applications*. 2023; 230: 120534.-DOI: https://doi.org/10.1016/j.eswa.2023.120534.
15. Kour P., Mansotra V. Implementation of pretrained models to classify osteosarcoma from histopathological images. *Proceedings of International Conference on Recent Innovations in Computing*. 2024; 589–603.-DOI: https://doi.org/10.1007/978-981-97-2839-8_41.
16. Bansal P., Gehlot K., Singhal A., et al. Automatic detection of osteosarcoma based on integrated features and feature

selection using a binary arithmetic optimization algorithm. *Multimed Tools Appl*. 2022; 81: 8807–8834.-DOI: https://doi.org/10.1007/s11042-022-11949-6.

17. Alabdulkreem E., Saeed M.K., Alotaibi S.S., et al. Bone cancer detection and classification using owl search algorithm with deep learning on x-ray images. *IEEE Access*. 2023; 11: 109095–103.-DOI: https://doi.org/10.1109/access.2023.3319293.
18. Alsubai S., Dutta A.K., Alghayadh F., et al. Group teaching optimization with deep learning-driven osteosarcoma detection using histopathological images. *IEEE Access*. 2024; 12: 34089–98.-DOI: https://doi.org/10.1109/access.2024.3371518.
19. Aydin Şimşek Ş., Aydin A., Say F., et al. Enhanced enchondroma detection from x-ray images using deep learning: A step towards accurate and cost-effective diagnosis. *Journal of Orthopaedic Research*. 2024; 42(12): 2826–34.-DOI: https://doi.org/10.1002/jor.25938.
20. Liu F., Zhu J., Lv B., et al. Auxiliary segmentation method of osteosarcoma MRI image based on transformer and U-net. *Comput Intell Neurosci*. 2022; 2022: 9990092.-DOI: https://doi.org/10.1155/2022/9990092.
21. Mohan B.C. Osteosarcoma classification using multilevel feature fusion and ensembles. 2021 IEEE 18th India Council International Conference (INDICON). 2021; 1–6.-DOI: https://doi.org/10.1109/indicon52576.2021.9691543.
22. Misaghi A., Goldin A., Awad M., Kulidjian A.A. Osteosarcoma: a comprehensive review. *SICOT J*. 2018; 4: 12.-DOI: https://doi.org/10.1051/sicotj/2017028.
23. Fu Y., Xue P., Ji H., et al. Deep model with Siamese network for viable and necrotic tumor regions assessment in osteosarcoma. *Med Phys*. 2020; 47(10): 4895-4905.-DOI: https://doi.org/10.1002/mp.14397.
24. Aljuaid H., Alturki N., Alsubaie N., et al. Computer-aided diagnosis for breast cancer classification using deep neural networks and transfer learning. *Computer Methods and Programs in Biomedicine*. 2022; 223: 106951.-DOI: https://doi.org/10.1016/j.cmpb.2022.106951.
25. Singh O., Kashyap K.L., Singh K.K. Lung and colon cancer classification of histopathology images using convolutional neural network. *SN Computer Science*. 2024; 5(2).-DOI: https://doi.org/10.1007/s42979-023-02546-x.
26. Aarthy R., Muthupriya V., Kalpana S., Ashok M.V. Bone cancer detection based on histopathology images using optimized temporal spatial multi scale dilated convolutional neural network with MultiNet. 2024 Advances in Science and Engineering Technology International Conferences (ASET). 2024; 01–8.-DOI: https://doi.org/10.1109/aset60340.2024.10708740.
27. Das S., Saikia J., Das S., Goni N. A comparative study of different noise filtering techniques in digital images. *International Journal of Engineering Research and General Science*. 2015; 3(5): 180.-ISSN: 2091-2730.-URL: https://pnrsolution.org/Datacenter/Vol3/Issue5/25.pdf.

Received / 11.02.2025
Reviewed / 10.04.2025
Accepted for publication / 19.06.2025

Author Information / ORCID

Sindudevi Jeevanandam / ORCID ID: https://orcid.org/0009-0008-0772-8332.
Muthaiya Govindarajan Kavitha / ORCID ID: https://orcid.org/0000-0001-6942-722X.